MANUFACTURING AND CHARACTERIZATION OF A CERAMIC SINGLE-USE MICROVALVE

Z. Khaji[1], L. Klintberg[1] and G.Thornell[1,2]
[1] *Div. of Microsystems Technology, Dept. of Engineering Sciences, Uppsala University, Uppsala, Sweden*
[2] *Ångström Space Technology Centre, Dept. of Engineering Sciences, Uppsala University, Uppsala, Sweden*

Email: zahra.khaji@angstrom.uu.se

Abstract — Presented here and with foreseen utilization in space applications and other demanding applications, is the manufacturing and characterization of a ceramic single-use microvalve with the potential to be integrated in lab on a chips. A-3 mm diameter membrane was used as the flow barrier, and the opening mechanism was based on cracking the membrane by inducing thermal stresses on it with fast and localized resistive heating.

Four manufacturing schemes based on high-temperature co-fired ceramic technology were studied.

Three designs for the integrated heaters and two thicknesses of 40 and 120 µm for the membranes were considered, and the heat distribution over their membranes, the required heating energies, their opening mode, and the flows admitted through were compared. Furthermore, the effect of applying +1 and -1 bar pressure difference on the membrane during cracking was investigated.

Thick membranes demonstrated unpromising results for low pressure applications since the heating either resulted in microcracks or cracking of the whole chip. Because of the higher pressure tolerance of the thick membranes, the design with microcracks can be considered for high-pressure applications where flow is facilitated anyway.

Thin membranes, on the other hand, showed different opening sizes depending on heater design and, consequently, heat distribution over the membranes, from microcracks to holes with the sizes of 3-100% of the membrane area. For all the designs, applying +1 bar over pressure, contributed to bigger openings, whereas -1 bar pressure difference had this influence just for one of the designs and resulted in smaller openings for the other two. The energy required for breaking these membranes was a few hundred mJ with no significant dependence on design and applied pressure.

The maximum sustainable pressure of the valve for the current design and thin membranes was 7 bar.

Keywords: **single-use valve, HTCC, alumina, platinum**

1. Introduction

One of the substantial building blocks of a successful miniaturized and fully integrated microfluidic system is reliable microvalves. Microvalves control the delivery of minute fluid amounts by flow regulation, on/off switching and sealing of liquids, gases or vacuums [1]. Several applications benefit from using isolation valves for hermetically sealed fluid storage and its on-demand delivery. In life sciences and chemistry, for instance, isolating biomolecules and chemical reagents is necessary for preventing reagents from contaminating each other and influencing the assays [2-3]. Automated fluid delivery has also been exploited for producing energy "on-demand" by feeding electrolytes into electrochemical cells [4-6].

Isolation valves also serve spacecraft industry, to a great extent, by sealing the propulsion system during long lead time on the ground before launch, and, more importantly, the very long travel time to the destination. This becomes of more importance for microspacecraft because their even higher waiting times demand the limited propellant supply to be conserved during long and inactive interplanetary cruises [7]. Single-use valves are often used in these applications since all multiple-use valves leak to some degree, and a small leakage in a microspacecraft can result in the loss of a significant portion of the propellant [7].

A MEMS, one-time use electrothermal valve with a Pt heater printed on top of a Parylene membrane is described in [8]. The power needed for heating was transferred wirelessly, which resulted in melting the membrane and, consequently, opening the valve within a few hundreds of milliseconds, using 22 mW in air and 33 mW in water. This low-power valve was suited for applications in wirelessly controlled implantable drug-delivery systems.

Another example of exploiting single-use valves in drug-delivery MEMS systems can be found in [9], where a variety of single-use paraffin-based microvalves made in a polycarbonate substrate were characterized. The actuation mechanism was based on the phase transition of paraffin in response to changes of the temperature. The maximum hold-up pressure, and the actuation power of these valves were 2.7 bar and 100- 200 mW, respectively, and their response time was in the order of tens of seconds.

Aiming at space industry, Bejhed *et al.* [10] have demonstrated a single-use valve made of Si for high-pressure applications. The valve was solder sealed and opened by re-melting the solder. The valve had an integrated heater and a filter to handle any particle debris created by the activation process. It was functional at pressures up to 100 bar, and opened in less than 10 s with an applied power of 13 W.

With application in microspacecraft, Jet Propulsion Laboratory (JPL) has developed a one-shot valve in which a narrow, doped silicon plug acts as the flow barrier [7]. When resitively heated, the plug melts and opens for the gas flow. Depending on the barrier thickness, JPL's valves tolerate pressures up to 206.8 bar, open in 0.1-0.3 ms, and consume at least 1-30 mJ of energy.

Presented in [11], is the evaluation of arrays of single-use valves, each consisting a thin metallic ohmic resistor patterned on a silicon nitride membrane. The membrane constitutes the flow barrier, and is made on a silicon wafer. Rapid heating via an electric pulse induces thermal stresses in the membrane/resistor, which in turn breaks the membrane and opens the valves. The valves withstood pressure differentials up to 5 bar and the required activation energies were from tens to hundreds of mJ.

In this work, a ceramic membrane with a heater printed on it is proposed as a one-time opening valve. Different schemes for manufacturing the valve using High-Temperature Co-fired Ceramic (HTCC) technology, as well as the feasibility of breaking it using rapid resistive heating are studied. The study also includes the influence of different heater designs, membrane thicknesses and pressure differences.

The interest in using HTCC in microsystems technology including microfluidics has recently increased due to its high temperature and chemical sustainability. For example microthrusters [12-13], microplasma sources [14], and a microcombustor for combusting solid minute samples prior to isotopic measurements of carbon [15], have been manufactured using HTCC. Integrating isolation valves in HTCC, is a step towards realizing a lab on a chip using this technology. Presented in [16], is an example of an ongoing effort to make an HTCC lab-on-a-chip for space applications. Among other components, this chip integrates the microplasma source and the microcombustor presented in [14] and [15], respectively, and is an application foreseen for the valve presented here.

2. Experimental

2.1. Design, materials and fabrication

A single-use opening valve consisting of a membrane with a heater pattern printed on it has been designed. The membrane acts as the flow barrier. The actuation mechanism exploits thermal stresses induced in the membrane by a localized temperature transient resulting from rapid resistive heating. The stresses cause the membrane to break and the flow to pass through, consequently.

The valve is made of two parts consisting of, in total, four ceramic layers: the membrane part (I) and the cavity stack (II), which in its turn is made of three layers with circular shaped cavities in the middle simulating a fluidic via, figure 1, left. These three layers also contribute to the mechanical robustness of the device.

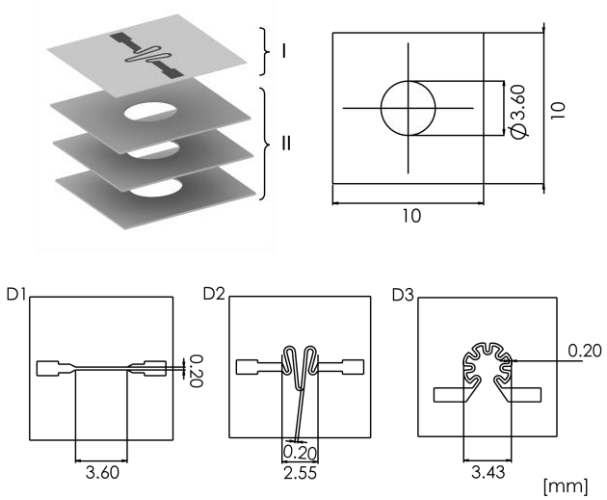

Figure 1. Exploded view of the valve (top, left) showing the membrane part (I) and the cavity stack (II), and the dimensions for design 1, 2 and 3 in mm before sintering (top right and bottom).

Three different patterns were designed for the heater: a line heater along the diameter of the membrane (design 1), a straight meander shape heater covering the surface of the membrane (design 2), and a curved meander shape heater covering the surface of the membrane just around the edges (design 3), figure 1, bottom. For each of the heater designs, a thin (40 µm) and a thick (120 µm) membrane were considered. For conciseness, hereafter, notations D1, D2, D3, Tk and Tn will be used for designs 1, 2, 3, thick and thin membranes, respectively.

Co-fired ceramic devices are commonly fabricated by processing individual layers of ceramic green tapes, stacking them into a 3-D structure, laminating them into each other, and firing all the constitutive materials at the same time.

In this work, the samples were manufactured from HTCC ceramic green tapes consisting of 99.99% alumina (ESL 44007‑50, 100, 150 µm, Electro Science Laboratories, USA). The conductive patterns were made by manually screen printing platinum paste (ESL 5571g, Electro Science Laboratories, USA) on the respective layers with a 325-mesh screen (Laser Technical Services A/S, Denmark) followed by drying for 15 min at 50ºC. The screen was designed so that 16 samples could be printed in each run. All the needed cuttings were done on the ceramic green tapes using a PCB plotter (Protomat S100, LPKF, Germany).

According to the manufacturer, the tapes had to be laminated at 20 MPa and 70 °C for 15 min. For mechanical support of the membranes during lamination and firing, the cavities were filled with a graphite fugitive (ESL 49000-125 µm, Electro Sciences Laboratories, USA) insert with the same shape and diameter as the cavities. Here, an in-house developed isostatic hydraulic press was used for lamination. The processed layers had to be aligned and stacked, and the stacking had to be vacuum packed prior to the lamination. For alignment, holes were milled in all the layers, which were then stacked between aluminum plates ($54 \times 54 \times 4$ mm^3) with alignment pins.

One should note the thickness difference between the ceramic and fugitive tapes which will cause a height difference between their respective stacks. This difference can have influence on the quality of the

manufactured membranes and the manufacturing yield. For this reason among others, four manufacturing methods were studied, which all had the above mentioned fundamental processes in common and differed mainly in the order of the manufacturing steps, as described in the following.

Method A was based on processing all the graphite and ceramic layers individually prior to the lamination. In this method, the cavity stack was made of 3 layers, each 150 µm thick, aligned using alignment pins. The cavities were manually filled with 3 single-tape graphite inserts. The lamination was then done in two steps, the first being a pre-lamination at 7 MPa and 60 °C for 10 min for the layers to stick to each other. Then the pressing was repeated at full nominal pressure, this time with the stacks placed between two aluminum sheets without alignment pins. This was done to avoid stresses that the pins could cause on the tapes at the high pressures, potentially resulting in damages.

Method B differs from method A mainly by pre-laminating the layers before machining them to study the influence of eliminating probable misalignments. Furthermore, by using 4 tapes for the fugitive inserts instead of 3, the height difference between the cavity and graphite insert was slightly decreased. The 3-layer cavity stack as well as the 4-layer stack of fugitive tapes were separately pre-laminated at 7 MP and 60 ºC. After lamination, the cavity and graphite stacks were milled through. The pre-laminated ceramic layers and a screen printed membrane layer were then aligned and the fugitive material inserted. Finally, lamination at full pressure was performed.

In order to further decrease the height difference between the stacks, Method C had two differences with method B. Its cavity stack was made of two 150 µm thick layers and one 100 µm thick layer, and the graphite stack included three layers instead of four.

Milling ceramic tapes usually leaves rough edges around the cavities, especially if it is done in an already laminated stack. This can affect the quality of membranes being laminated to these cavities. Furthermore, since laminating screen printed tapes will press the printed pattern into the ceramic tape, this can change the quality and yield of the components, and therefore should be studied. Method D is included to study these effects are studied. In this method, after milling the cavities in the pre-laminated ceramic stack and adding the fugitive inserts in the same manner as method C, a further pressing step at 2.5 MPa and 70 ºC for 10 min was introduced. During the lamination, the cavity stack was placed between the ceramic carrier film on one side, and an aluminum sheet on the other side. The aim of the extra pressing step was smoothing the edges of the cavities slightly by pressing against the plastic carrier film. After this, an unprocessed tape was laminated to the smooth part of the stack at full pressure. Screen printing of the heater patterns was done after the full lamination. By printing after pressing in method D, and comparing the results with the other methods, which entailed pressing after printing, one can investigate the influence of pressing a printed metal into a membrane.

Eventually, and for all the methods, the production was completed by cutting the contours of the individual samples followed by firing according to the manufacturer's recommendation. A full description of the sintering profile can be found in [15]. Table 1 summarizes the main differences between methods A-D.

Table 1. Summary of the differences between methods A to D

Method	Thickness of the cavity stack	Thickness of the graphite stack	Order of manufacturing steps
A	450 µm	375 µm	Milling and printing/ pre-lamination/full lamination
B	450 µm	500 µm	Pre-lamination/ milling and printing/full lamination
C	400 µm	375 µm	Pre-lamination/ milling and printing/full lamination
D	400 µm	375 µm	Pre-lamination/ milling/intermediate pressing /full lamination/ printing

2.2. Characterization

2.2.1. Inspection

The dimensions of the samples after sintering were measured using a digital caliper and a thickness measurement gauge.

The quality of the completed samples was inspected using optical microscopy and X-ray microscopy (XT V 130, Nikon, Japan).

The resistances of the heaters were measured using a hand-held digital multimeter (Fluke, 115 True RMS, USA).

The membranes were also inspected for cracks and leakages after manufacturing, by inserting a few droplets of ink dissolved in water into the cavity. Due to the hydrophilicity of alumina, traces of ink would be seen on the other side of membrane in case cracks exist.

2.2.1. Performance evaluation

The main principle behind the characterization was to resistively heat the membranes with the maximum possible power and in the shortest possible time, in order to localize the heat in the membranes and avoid conducting the heat through the whole chip. The behavior of the membrane was studied during the heating.

Figure 2 illustrates the measurement set-up. A desk power supply (QL355P, TTi, UK) was used for the resistive heating. The measuring instruments were a high-speed camera (Phantom Miro M310, Vision Research, USA) for filming through an optical microscope, an IR camera (Thermovision A40, FLIR Systems, Sweden) for studying the heat profile over the membranes during heating, and a digital oscilloscope (DSO7104A, Agilent, USA) for measuring the power consumed over time. A 1-Ω resistance (ten 10-Ω resistors in parallel) was used in series with the samples for measuring the consumed current using the oscilloscope.

For holding the samples during measurements, a fixture with a hole in the middle was made from PCB, figure 3. Using silver conductive epoxy (CW2400, Chemtronics, USA), 200 µm thick silver wires were connected to the heaters of each sample. These wires were then soldered to the connection pads of the fixture. Having done so, the samples were hanging from their wires in air during the measurements. The fixture was clamped to an XYZ table for fine positioning of the samples with respect to the cameras, with the membrane facing the high-speed camera and the cavity stack facing the IR camera. MATLAB was used for computer control of the set-up.

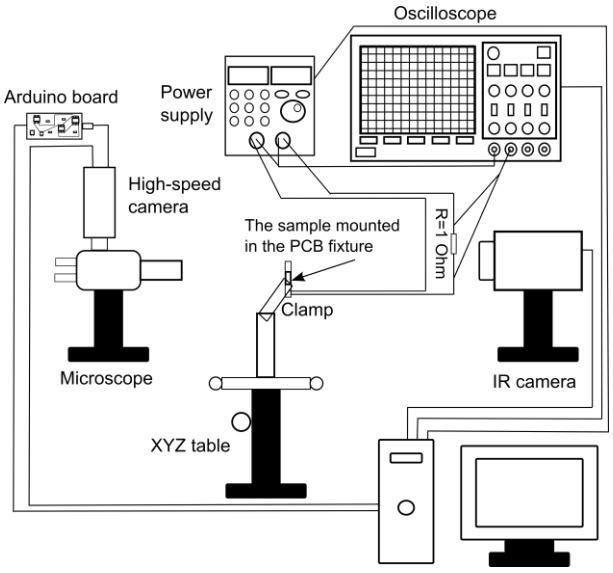

Figure 2. Block diagram of the measurement set-up

An image resolution of 384×288, a sampling rate of 10000 frames per second, an exposure time of 99 µsec and a footage duration of 7.679 s were the parameters used for the high-speed camera. The image resolution was governed by the dimensions of the membranes, and the sampling rate was the maximum possible for the resolution and light intensity used. The high-speed camera was triggered through a MATLAB program by using a micro-controller board (Uno A000066, Arduino, Italy).

The IR camera was set to capture pictures at highest possible rate of 12.5 Hz. In this manner, 6 samples of each of the design batches were characterized.

The power supply was set to deliver the maximum voltage and current of 20 V and 3 A as fast as possible for the instrument, being within 20 ms). The feasibility of this was confirmed by thermal stress and heat transfer simulations performed with COMSOL Multiphysics 4.3 b. In these, the possibility of achieving thermal stresses above the yield strength of alumina on the membrane under these conditions was studied. That the heat was mainly localized in the membrane and not dissipated to the other parts of the component was also verified by the modelling.

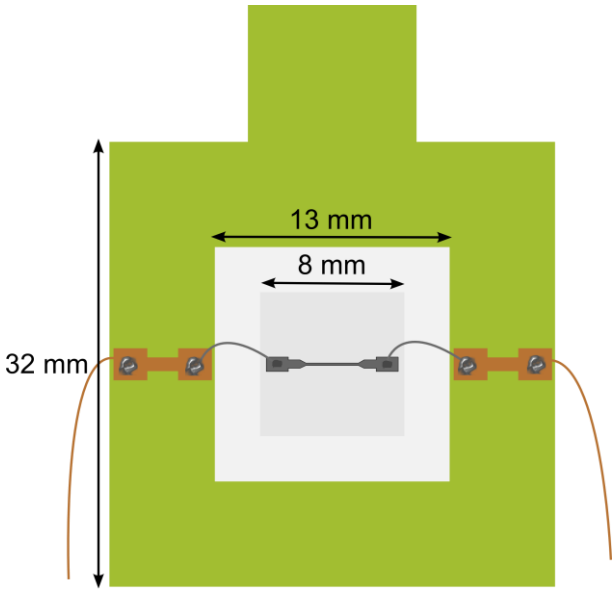

Figure 3. Schematic of the PCB fixture with dimensions. The sample was suspended in the middle hole by its wires soldered to the PCB's connection pads. Longer wires were soldered to other side of these pads to facilitate connection to instruments.

In order to study the influence of pressure difference on the performance of the valves, samples of type D1_Tk, D1_Tn, D2_Tn and D3_Tn were chosen to be characterized under a pressure difference. The reason for exclusion of samples D2_Tk and D3_Tk from this study will be given in part 3.

Tubes of 6 mm diameter (PA12 PL 6×1, Bosch Rexroth, Germany) were glued to the back of the chips and around the cavities using epoxy glue (Araldite 2000, Huntsman, USA). Pressure differences of +1 bar and -1 were implemented by connecting the hoses to a nitrogen gas container and a diaphragm vacuum pump (LABOPORT, KNF, Germany), respectively. In order to ensure that the desired pressure conditions were met, two sensors were used: a pressure sensor (S model, Swagelok, USA) for overpressure and a Penning gauge (CP25-K, Edwards, UK) for vacuum. Before doing the experiment, pressure endurance tests were done on 6 samples (4 Tn and 2 Tk samples) in order to assure that cracking the membranes just by applying the aimed at pressures was not possible.

No thermography was done during the pressure characterizations since the back sides of the membranes were covered by the hoses. Furthermore, the PCB fixture was not used during these experiments. Instead, long wires were glued directly to the heaters using the silver epoxy. From each of the batches, 6 samples were chosen, 3 of which were characterized at +1 bar and 3 at -1 bar.

Finally, a flow test was carried out on the opened valves for investigating the size of the openings. This was done by pressurizing membranes from one side and measuring the flow passing through by use of a mass flow sensor (0-1000 sccm, Honeywell International Inc., USA). Pressurization was done in the same manner as described above, but with the applied over pressure of +33 mbar as limited by the maximum measurable flow rates possible by the sensor for the biggest openings.

3. Results

3. 1. Manufacturing results

Figure 4 shows an example of an X-ray microscopy image of a D2 valve manufactured using method A after sintering. The membrane can be distinguished by its lighter color. One can also see a slight misalignment between the cavity layers as the result of using alignment pins. This misalignment was not

observed in samples manufactured using methods B-D, where no alignment was needed for the cavity stack.

The average shrinkage of the samples after sintering in xy and z directions was 18% and 20%, respectively.

The heaters of D1, D2 and D3 had the respective average resistances of 0.9, 2.1 and 2.2 Ω with the standard deviations of 0, 0.2 and 0.7 Ω.

Manufacturing methods A-D resulted in different yields for different designs, table 2. Note that all the designs were not manufactured with all the methods due to results from preliminary membrane opening tests.

Table 2. Yields of different manufacturing methods for different designs, as the ratio of flawless samples to the number of samples manufactured.

Method	D1_Tn	D2_Tn	D3_Tn	D1_Tk	D2_Tk	D3_Tk
A	0/16	0/16	0/16	8/16	9/16	3/16
B	0/16	0/16	0/16	14/16	-	-
C	16/16	0/16	0/16	-	-	-
D	-	16/16	16/16	-	-	-

Using method A resulted in 0% yield for thin membranes as small cracks were observed around the membrane edges. Using the ink test, leakages were observed through many of these cracks. For the samples with thick membranes, the cracks were seen in 50-81 % of the samples.

Method B also had 0% yield for the thin membranes. On the other hand, it improved the yield for D1_Tk samples to 87%.

Although method C was successful, manufacturing D1_Tn samples with 100% yield, it showed no success in making D2 and D3 thin samples.

By exploiting method D, 100% yield was achieved in making D2_Tn and D3_Tn samples.

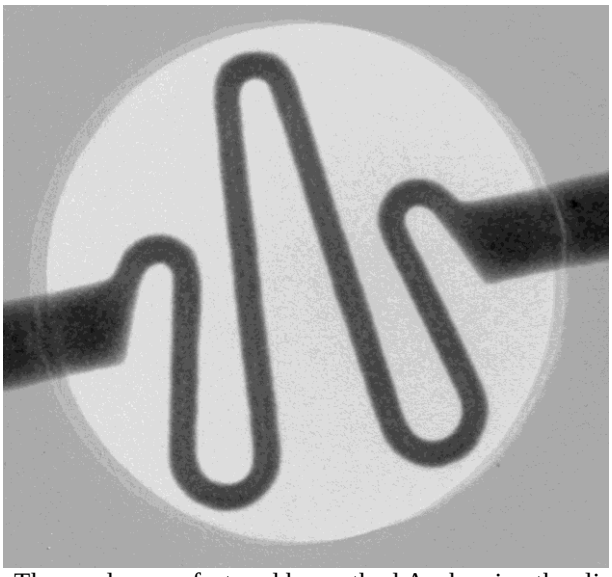

Figure 4. X-ray image of D2_Tk sample manufactured by method A, showing the slight misalignment between the cavity layers.

3.2. Performance evaluation result

3.2.1. Thermography results

From figure 5, one can see that for the D1 sample, more heat is localized in the middle part of the membrane, especially in the middle of the heater, whereas for the D2 sample, the heat is more evenly distributed over the membrane. For the D3 sample, on the other hand, the hottest spots are found is a band around the edges.

The sampling rate of the IR camera was not enough for recording of the whole opening process, especially for thin membranes with their shorter breaking time. Therefore, estimating the maximum temperatures of the membranes just before breaking was not possible.

3.2.2. Valve opening results

It was observed that regardless of the heater design, high contact resistances, as well as high local resistance as the result of low quality of screen printing, contributed to local heating around the high resistance area which resulted in local melting of Pt and disconnecting the heater. This was more critical for D1 samples due to their lower resistances. The results from those samples (3 samples in total) are considered as outliers and are therefore not presented here.

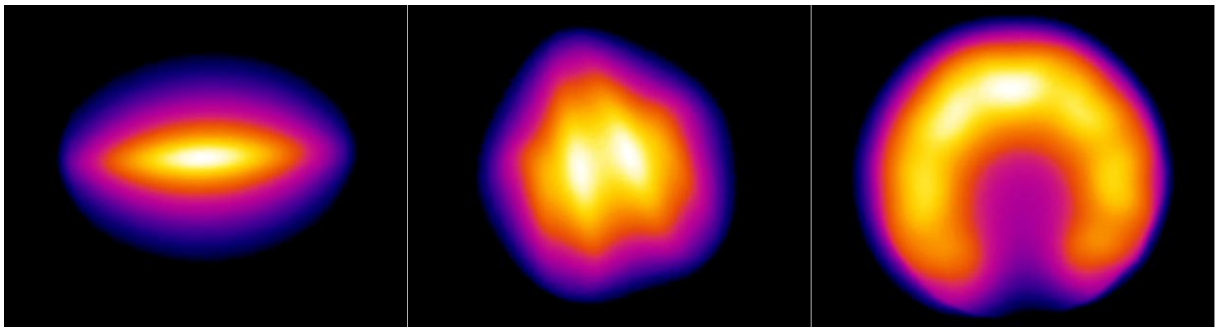

Figure 5. IR image of a D1_Tk (left), D2_Tk (middle) and D3_Tk (right) sample during resistive heating. The pictures were the last ones taken before breaking and were adjusted for the emissivity of alumina. Brighter colors are indicative of higher temperatures.

Tk membranes tolerated the maximum applicable pressures of 8 bar. Tn membranes on the other hand, sustained pressures between 3 and 7 bar.

Resistive heating of samples with thick membranes essentially gave two different results: cracking of the whole chip, or local melting of the heater with some microcracks around it. For D2_Tk and D3_Tk samples, the result was cracking of the whole chip. Figure 6 shows 4 frames from the high-speed camera footage of one of these samples. This makes these valve designs uninteresting for lab-on-a-chip applications, wherefore they were not further included in the experiments.

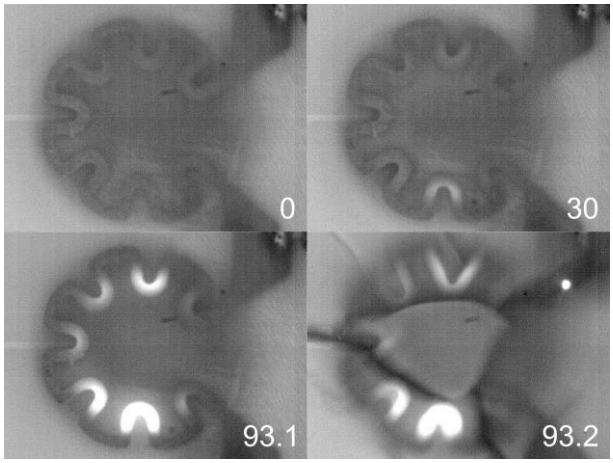

Figure 6. Frames from the high-speed camera video of a D3_Tk sample. Elapsed time in msec is displayed on each frame. The membrane appears darker as the result of the ink test done before this experiment.

D1_Tk samples, on the other hand, showed totally different results by the heaters being locally melted around the middle of the pattern. Microcracks were observed in the membranes after the experiment, mainly along the heater pattern and near the melted area, figure 7. Applying +1 or -1 bar pressure difference on the membrane did not change the result.

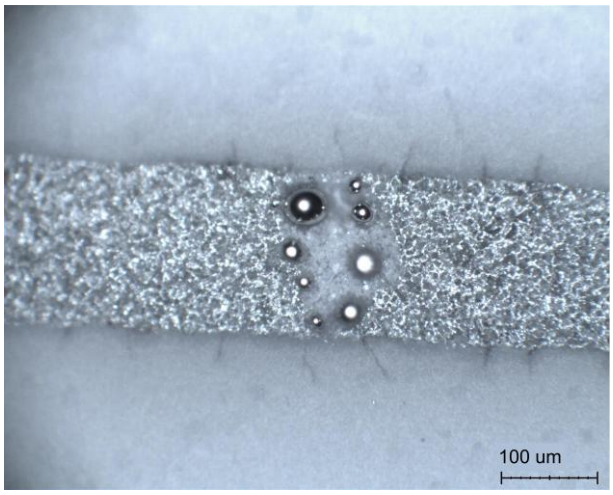

Figure 7. Part of a heater of a D1_Tk sample after heating. The heater was locally melted in the middle. Microcracks perpendicular to the heater are also visible.

For all the Tn samples, fast heating resulted in one of five general opening modes, table 3.

Table 3. Modes of Tn valve openings and the flows passing through afterwards. An over pressure of 33 mbar was applied during the flow measurements.

Mode	Description	Quantification	Flow (sccm)
1	The whole membrane detached	-	≥ 1000
2	Major part of the membrane detached	70-90% of the membrane area was opened.	≥ 1000
3	A hole in the membrane	3-30% of the membrane area was opened.	≥ 1000
4	A crack/cracks in the membrane	Crack lengths were between a few hundred µm to the diameter of the membrane.	23-322
5	Local melting of heater + microcracks	-	0-27

In figure 8, one can see the occurrence of each mode for designs 1-3 at different pressure differences.

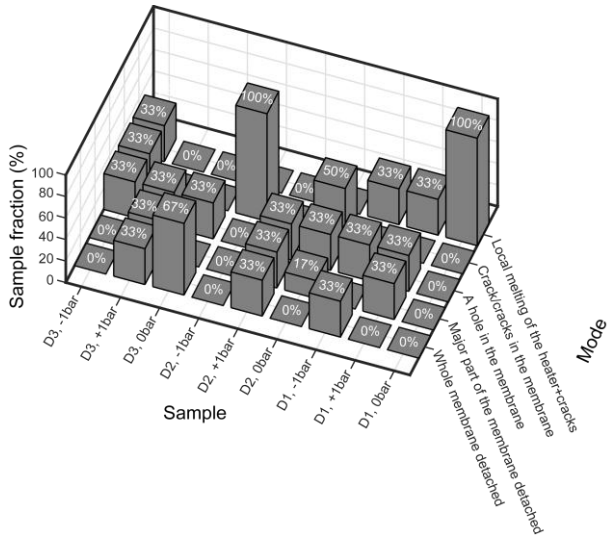

Figure 8. Opening mode distribution of different Tn sample designs under different pressure conditions.

As shown in figure 8, at 0 bar pressure difference, D1_Tn samples showed the same melting of the heater in combination with microcracks as observed for the D1_Tk ones. But in this case both +1 and -1 bar pressure differences for 66% of the samples contributed to bigger openings (modes 1-3) in the membrane. The sizes of the openings varied a lot between different samples.

50% of the D2_Tn samples had got holes in the membrane at zero pressure difference while the others got millimeter long cracks. Applying +1 bar pressure difference, contributed to much bigger openings. At -1 bar on the other hand, no hole was created and just big cracks were observed.

It is seen that at zero pressure difference, for all the D3_Tn samples, the whole membrane was detached or a hole was created (modes 1 or 3). The same behavior was observed at +1 bar pressure difference. At -1 bar, on the other hand, different sizes of openings were created and no general trend was observed.

In figures 9 and 10, some frames from the video recorded by the high-speed camera during resistive heating of chosen samples from batches D2_Tn and D3_Tn are shown. The chosen samples, had the dominant mode of their own batch after the heating *e.g.*, the sample chosen from batch D3, had the whole membrane detached after heating

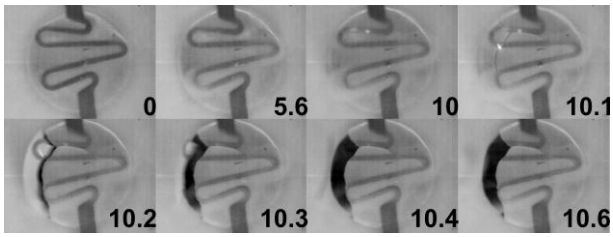

Figure 9. Frames from the high-speed camera footage of a D2_Tn sample. Elapsed time in ms is displayed on each frame.

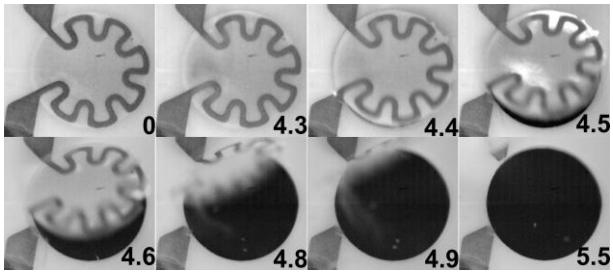

Figure 10. Frames from the high-speed camera footage of a D3_Tn sample. Elapsed time in ms is displayed on each frame.

From figures 9 and 10, it is clear that the actual breaking time is so short that studying the fracturing in detail is almost impossible with the frame rate of the camera.

The energy needed for cracking Tk samples varied between 2 and 10 J.

Figure 11 compares the energy needed for breaking D1-3 Tn membranes at pressure differences of 0, +1 and -1 bar.

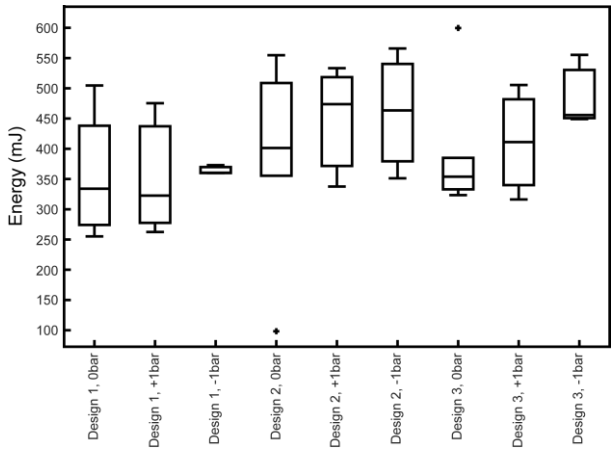

Figure 11. Comparison of the energies consumed for opening D1-3 Tn membranes at different pressure differences. Two Separate marks in the figure indicate outliers.

The energy needed for breaking Tn membranes were in the range of 250 to 560 mJ. No significant difference in the required energy was observed between different designs, and no trend in energy consumption as the result of applying pressure differences could be resolved.

The flow through all the cracked D1_Tk samples was measured to be zero at the applied over pressure of 33 mbar. On the other hand, almost all these cracked samples with zero flow, showed leakages during ink test.

Table 3 demonstrates the flows passing through all the broken Tn membranes being pressurized at 33 mbar over pressure. Modes 1-3 showed almost no deviation in the flow measurements and even openings as small as 3% of the membrane area was enough to pass high flows. One should note that for these modes, the flow sensor had reached its maximum measurable value of 1000 sccm and the actual flow can be any value above that. The samples with mode 4, *i.e.*, cracks on the membrane, had the most deviations in the flow varying from 23 to slightly above 300 sccm. Samples with mode 5 showed small deviations around low values of measured flows.

As with the D1_Tk samples, ink leaked through the microcracks in D1_Tn samples even though the flow measured was negligible.

4. Discussion and future work

4. 1. Manufacturing

One reason for the cracks observed around the edges of membranes resulting from the manufacturing, can be related to the thickness difference between the cavity and graphite stacks. This difference can cause the membrane to deflect during pressing, and potentially damage it. It is clear that this effect can be more significant for thin membranes. This difference and its consequent damages on membranes decreases from method A to D. It should be mentioned that the misalignments observed between three cavity layers in samples manufactured using method A could aggravate this problem since the misalignments could contribute to imperfect placement of the inserts, which, in turn, can further increase the height differences in some places.

Three potential reasons could be related to the success of method D in manufacturing D2_Tn and D3_Tn samples. One was minimizing the thickness difference between ceramic and graphite stacking. The second was smoothing the edges of the cavities by the extra pressing step as mentioned in part 2.1. It is believed that laminating a thin membrane on top of a sharp edge at high pressures may cause the membrane to crack. In addition to this, since the same manufacturing process resulted in different qualities for different metal patterns, one can relate the problem to pressing after screen printing. During lamination, a screen printed pattern is pressed into the ceramic tape. A metal pattern with a thickness

comparable with the thickness of the tape is pressed relatively far into the tape, and this can cause cracks around the membrane edges which are already the weakest part. The larger the area of the metal pattern is, and the closer the metal pattern is to the edges, the worse the problem becomes. This explains why making tight D1_Tn samples was possible by using method C, whereas D2_Tn and D3_Tn with more metals had cracks. Hence, by printing after pressing, method D conquered this problem.

Based on the initial cracking results, improving the yield of manufacturing D2 and D3 Tk samples was not deemed worthwhile, and therefore they were not manufactured using methods B to D. Based on the results seen for Tn samples, one can expect great yield improvements also for these samples if they had been manufactured using methods C and D, especially as thicker membranes are not as sensitive for manufacturing imperfections as thinner ones.

The deviations in the resistances of the heater patterns can be related to varying qualities of screen printing. It should be mentioned that the best quality of screen printing is achieved when the pattern to be printed is in parallel with the direction of the screen's wires. Although straightforward for a linear pattern, this is not possible for meander shapes. This explains the increasing deviations of the resistances from design 1 to 3.

4. 2. Characterization

Generalizing the thermography results (figure 5) for the Tn samples and taking figure 8 into consideration, one can relate the mode of openings created in the membrane at 0 bar pressure difference to the heat distribution during heating. Therefore, D1 membranes with most of the heat localized in the center, had their heaters locally melted around its middle. On the other hand D2 samples with heat more evenly distributed over the membrane, got openings with different sizes in different places of the membrane. The whole membrane of 67% of D3 samples was detached as the heat was mainly localized to the edges of the membrane.

It is worth mentioning that apart from material properties, the maximum sustainable pressure of the membrane depends on its geometry, and therefore, by re-dimensioning the membrane, *e.g.*, decreasing its diameter, one can increase the maximum tolerable pressure.

Both of the possible opening modes for Tk samples, made them uninteresting for their foreseen applications. D1 samples just got microcracks and not an opening, and D2 and D3 samples had their whole chips cracked, which makes their integration into lab on a chips inappropriate.

At 0 bar, D1_Tn samples had the same opening modes as the D1_Tk ones, with no significant flows passing through. Hence, this design is not promising for a valve application. Since for almost all the D1 samples, despite the flow measurement results, ink test indicated leakage, one can expect non-zero flows even for D1 valves at higher applied pressure differences. Applying +1 and -1 bar, resulted in 2/3 of the D1 samples getting openings rather than microcracks.

Great deviations in flows measured from samples with cracks (table 3) decrease their reliability as valves. Therefore Design 2 with 50% and 100% of its samples operating in this mode at 0 bar and -1 bar, will have lower reliability in valve applications. Furthermore, the flows were much smaller than samples with modes 1-3, and higher pressures might be needed for passing higher flows. Breaking D2 samples at +1 bar difference on the other hand, resulted in openings and no membranes with just cracks were observed.

Samples with D3 heaters, on the other hand, had the most reliable behavior at zero pressure difference and had got big openings which permitted high flows to pass through even for gases at low pressures. At +1 bar pressure difference, all the samples still had openings, whereas at -1 bar, different results from cracks to openings were observed which will decrease the reliability in their performance.

4. 3. Future work

Although applying +1 bar pressure difference mainly contributed to bigger openings, -1 bar pressure difference had this effect just for D1 samples and contributed to some smaller openings for D2 and D3. Therefore, the influence of pressure difference has to be further investigated in the future.

Regardless of design and pressure, development of integrated filters for collecting the particles produced during the breaking is important for applications of the valves in a lab on a chip.

5. Conclusions

Of the four methods presented here, method D (*i.e.*, milling and printing of pre-laminated sheets) showed the best qualities for the thin membranes. Even though this method was just used for two of the

designs and for the thin membranes, there is no indication that it should not show equally good results for the other designs and thicknesses.

As the current sustainable pressure of the valves (maximum of 7 bar for the thin membranes) can be increased by modifying the dimensions of the membrane, the valves can be potentially used to isolate fluids at higher pressures than the ones presented here.

Despite the linear heater (D1) resulting just in microopenings, one could consider using it for thick-membrane valves in applications where a high pressure of the fluid will facilitate enough flow through a small opening.

For thin-membrane valves, the curved meander heater (D3) exhibits more reliable results and bigger openings after breaking, than valves with the straight heater meander.

Low energies (few hundred mJ for the thin membranes) consumed for opening the valves, regardless of the design and pressure difference, make them suitable for applications where limited energy is accessible.

Acknowledgements

The Centre for Natural Disasters Science (CNDS) and the Swedish National Space Board are acknowledged for project funding. The Knut and Alice Wallenberg foundation is acknowledged for funding the laboratory facilities.

The generosity of time, knowledge and equipment from Jan-Åke Gustafsson at the Microstructure Laboratory, and Martin Berglund and Anders Persson at the Department of Engineering Sciences at Uppsala University is highly appreciated.

References

[1] K. W. Oh and C. H. Ahn, "A review of microvalves," *J. Micromechanics Microengineering*, vol. 16, no. 5, p. R13, 2006.

[2] A. J. Tudos, G. J. Besselink, and R. B. Schasfoort, "Trends in miniaturized total analysis systems for point-of-care testing in clinical chemistry.," *Lab Chip*, vol. 1, no. 2, pp. 83–95, Dec. 2001.

[3] M. A. Schwarz and P. C. Hauser, "Recent developments in detection methods for microfabricated analytical devices.," *Lab Chip*, vol. 1, no. 1, pp. 1–6, Sep. 2001.

[4] K. B. Lee and L. Lin, "Electrolyte-based on-demand and disposable microbattery," *J. Microelectromechanical Syst.*, vol. 12, no. 6, pp. 840–847, Dec. 2003.

[5] A. M. Cardenas-Valencia, J. Dlutowski, S. Knighton, C. J. Biver, J. Bumgarner, and L. Langebrake, "Aluminum-anode, silicon-based micro-cells for powering expendable MEMS and lab-on-a-chip devices," *Sensors Actuators B Chem.*, vol. 122, no. 1, pp. 328–336, Mar. 2007.

[6] A. M. Cardenas-Valencia, V. R. Challa, D. Fries, L. Langebrake, R. F. Benson, and S. Bhansali, "A micro-fluidic galvanic cell as an on-chip power source," *Sensors Actuators B Chem.*, vol. 95, no. 1–3, pp. 406–413, Oct. 2003.

[7] J. Mueller, C. Marrese, J. Polk, E.-H. Yang, A. Green, V. White, D. Bame, I. Chadraborty, and S. Vargo, "An overview of MEMS-based micropropulsion developments at JPL," *Acta Astronaut.*, vol. 52, no. 9–12, pp. 881–895, May 2003.

[8] P.-Y. Li, T. K. Givrad, D. P. Holschneider, J.-M. I. Maarek, and E. Meng, "A Parylene MEMS Electrothermal Valve.," *J. Microelectromech. Syst.*, vol. 18, no. 6, pp. 1184–1197, Dec. 2009.

[9] R. Liu, "Single-use, thermally actuated paraffin valves for microfluidic applications," *Sensors Actuators B Chem.*, vol. 98, no. 2–3, pp. 328–336, Mar. 2004.

[10] J. Bejhed, P. Rangsten, and J. Köhler, "Demonstration of a single use microsystem valve for high gas pressure applications," *J. Micromechanics Microengineering*, vol. 17, no. 3, p. 472, 2007.

[11] A. M. Cardenas-Valencia, J. Dlutowski, J. Bumgarner, C. Munoz, W. Wang, R. Popuri, and L. Langebrake, "Development of various designs of low-power, MEMS valves for fluidic applications," *Sensors Actuators A Phys.*, vol. 136, no. 1, pp. 374–384, May 2007.

[12] V. Lekholm, A. Persson, K. Palmer, F. Ericson, and G. Thornell, "High-temperature zirconia microthruster with an integrated flow sensor," *J. Micromechanics Microengineering*, vol. 23, no. 5, p. 55004, 2013.

[13] K. H. Cheah and K.-S. Low, "Fabrication and performance evaluation of a high temperature co-fired ceramic vaporizing liquid microthruster," *J. Micromechanics Microengineering*, vol. 25, no.

1, p. 15013, 2015.
[14] M. Berglund, A. Persson, and G. Thornell, “Evaluation of Dielectric Properties of HTCC Alumina for Realization of Plasma Sources,” *J. Electron. Mater.*, vol. 44, no. 10, pp. 3654–3660, Jul. 2015.
[15] Z. Khaji, P. Sturesson, L. Klintberg, K. Hjort, and G. Thornell, “Manufacturing and characterization of a ceramic microcombustor with integrated oxygen storage and release element,” *J. Micromechanics Microengineering*, vol. 25, no. 10, p. 104006, 2015.
[16] A. Persson, M. Berglund, Z. Khaji, P. Sturesson, J. Söderberg, and G. Thornell, “Optogalvanic spectroscopy with microplasma sources – Current status and development towards lab on a chip,” *J. Micromechanics Microengineering*, 2016.